Journal of Cellular Biochemistry 84:173–187 (2002)

Characterization of G3BPs: Tissue Specific Expression, Chromosomal Localisation and *ras*GAP^{120} Binding Studies

Derek Kennedy,[1,2]* Juliet French,[1] Estelle Guitard,[3] Kelin Ru,[1] Bruno Tocque,[3] and John Mattick[1]

[1]The Institute for Molecular Bioscience and the Department of Biochemistry, University of Queensland, Brisbane, Queensland, Australia
[2]School of Biomolecular and Biomedical Science, Griffith University, Brisbane, Queensland, Australia
[3]ExonHit Therapeutics, France

Abstract The G3BP (*ras*-GTPase-Activating Protein SH3-Domain-Binding Protein) family of proteins has been implicated in both signal transduction and RNA-metabolism. We have previously identified human G3BP-1, G3BP-2, and mouse G3BP-2. Here, we report the cloning of mouse G3BP-1, the discovery of two alternatively spliced isoforms of mouse, and human G3BP-2 (G3BP-2a and G3BP-2b), and the chromosomal localisation of human G3BP-1 and G3BP-2, which map to 5q14.2-5q33.3 and 4q12-4q24 respectively. We mapped the *ras*GAP^{120} interactive region of the G3BP-2 isoforms and show that both G3BP-2a and G3BP-2b use an N-terminal NTF2-like domain for *ras*GAP^{120} binding rather than several available proline-rich (PxxP) motifs found in members of the G3BPs. Furthermore, we have characterized the protein expression of both G3BP-1 and G3BP-2a/b in adult mouse tissues, and show them to be both tissue and isoform specific. J. Cell. Biochem. 84: 173–187, 2002.

Key words: RRM; SH3; RNA binding protein; signal transduction

RNA processing is an integral part of cellular metabolism controlled through pre-mRNA splicing, RNA transport, and RNA stability [Dreyfuss et al., 1996]. Regulation of RNA metabolism has been shown to play an important role in development. Notable examples are the cascade of alternative RNA splicing events initiated by *sex-lethal* in *Drosophila* sex determination and dosage compensation [Bopp et al., 1996], and the roles of *elav* and *musashi* in neural development in both *Drosophila* and the mouse [Sakakibara et al., 1996]. Abnormal functions or distribution of RNA-binding proteins have also been implicated in human disorders, such as the Fragile X syndrome [Siomi et al., 1993] and myxoid liposarcoma [Crozat et al., 1993]. Recently, there has been increased interest in the control of mRNA translation mediated by RNA-binding proteins, in particular the role of these proteins in 5′ UTR interactions that influence elongation factors [Svitkin et al., 1996] as well as 3′ interactions involving translational activity [Dreyfuss et al., 1996] and degradation [Gallouzi et al., 1998]. It is important to characterize the mechanisms that allow RNA-binding proteins to respond to environmental and developmental signals through transduction cascades in order to understand their role in human diseases.

Ras-GTPase activating protein (*ras*GAP^{120}) is an important regulator of signal transduction [Pomerance et al., 1996], which sits at the nexus of positive and negative control of the oncogene *ras*. The *ras* or p^{21} molecule is a guanine nucleotide binding protein implicated in activation of downstream signaling kinase pathways [van der Geer et al., 1997]. *ras*GAP^{120} itself stimulates the hydrolysis of GTP bound *Ras* (reviewed in Tocque et al., 1997) and thereby regulates the activity of *ras*. The catalytic GTP

Derek Kennedy and Juliet French contributed equally to the preparation of this manuscript.

*Correspondence to: Derek Kennedy, School of Biomolecular and Biomedical Science, Griffith University, Nathan, Queensland, Australia 4111.
E-mail: Derek.Kennedy@mailbox.gu.edu.au

Received 22 September 1999; Accepted 24 July 2001

DOI 10.1002/jcb.1277

hydrolysing domain of *ras*GAP^{120} lies in its carboxy-terminus [Tocque et al., 1997], whereas the amino-terminus contains a calcium-dependent lipid binding domain, a pleckstrin homology domain and an SH3 domain flanked by two SH2 domains [Tocque et al., 1997]. The N-terminal Src homology domains of *ras*GAP^{120} have been implicated in an effector-like activity however, the mechanism of this activity has not yet been characterized. The functional importance of the *ras*GAP^{120} SH3 domain has been demonstrated by use of antibodies specifically raised to the SH3 domain of *ras*GAP^{120}. It was demonstrated in vivo that this domain is important in organisation of the cellular cytoskeleton stimulated by growth factors or activated *ras* [Leblanc et al., 1998], in Cdc2 activation, and Mos induction [Pomerance et al., 1996], and germinal vesicle breakdown in *Xenopus* oocytes [Duchesne et al., 1993].

Human *ras*-GTPase-Activating Protein SH3-Domain-binding Protein (G3BP-1) was first identified by its co-immunoprecipitation with *ras*GAP^{120} using an amino-terminal construct of *ras*GAP^{120} [Parker et al., 1996]. G3BP was the first protein shown to bind the *ras*GAP^{120} SH3 domain, however other *ras*GAP^{120} SH3-binding proteins have since been reported, including a 14 kDa protein [Hu and Settleman, 1997], and the huntingtin protein [Liu et al., 1997]. Genetic studies in *Drosophila* support a role for G3BP in *ras* signaling [Pazman et al., 2000]. Mutations in *Drosophila* G3BP, known as *rasputin* (*rin*), show defects in photoreceptor recruitment and ommatidial polarity in the eye. *Rin* mutants were shown to function downstream of *ras* but independent of the Raf/MAPK pathway. Furthermore, a genetic interaction between Rin/G3BP and RhoA was shown suggesting that Rin/G3BP may provide the link between Ras and Rho signaling pathways.

We cloned and sequenced mouse G3BP-2 as part of a general screening for RNA recognition motif (RRM)-containing proteins [Kennedy et al., 1997], and recently cloned the human homologue of this gene. Primary sequence analysis of G3BPs also indicated that they contain an RNA recognition motif (RRM) [Nagai et al., 1995], an RGG domain [Burd and Dreyfuss, 1994; Siomi and Dreyfuss, 1997], and a nuclear transport factor 2-like (NTF2-like) domain [Suyama et al., 2000]. RRMs are structural domains that are readily identified by two signature sequences, an octapeptide referred to as RNP-1, and a hexapeptide, RNP-2. In the three dimensional structure of the RRM, the two signature sequences form the two inner beta strands of a overall structure that contains a four strand anti-parallel beta sheet, and two alpha helices in a β-α-β-β-α-β conformation [Nagai et al., 1995]. The four strand beta sheet provides a platform from which aromatic side chains can interact with RNA targets consistent with the requirements for ring stacking interactions [Nagai et al., 1995]. The proposed structure of the RRM in G3BP has been reported elsewhere [Kennedy et al., 1997]. The G3BPs also contain acid-rich and RGG domains, which are often considered auxiliary domains for RRM-type RNA-binding proteins [Burd and Dreyfuss, 1994; Siomi and Dreyfuss, 1997]. The RGG domain consists of closely spaced arginine-glycine-glycine repeats that form a flexible helical β spiral. Residues interspersed within the repeats are thought to be responsible for RNA interactions through ring stacking with aromatic side chains, or hydrogen bonding to bulky side chains (reviewed in Burd and Dreyfuss, 1994). These structural motifs are consistent with the recent finding that G3BP-1 is implicated in RNA metabolism by acting in vitro as a cleavage factor for *c-myc* transcripts [Gallouzi et al., 1998]. G3BP-1 has also been isolated from the nuclear fraction of HeLa cells, and characterized as having a helicase activity on DNA, and RNA/DNA or RNA/RNA duplexes [Costa et al., 1999] however, the biological significance of these functions are yet to be elucidated. Previously, another RNA binding protein, containing RRMs and RGG domains, was also characterized as a helicase, and was identified as nucleolin [Tuteja and Tuteja, 1998].

The NTF2 protein facilitates nuclear import of RanGDP and maintains a Ran gradient across the nuclear membrane. The Ran gradient is responsible for cargo uptake and release from transport receptors such as importins and exportins. Once in the nucleus, RanGDP is converted to RanGTP by the nucleotide exchange factor RCC1 causing a dissociation of NTF2. Subsequently, RanGTP complexed to import receptors recycles back to the cytoplasm, RanGTP is then hydrolysed by RanGTPase activating protein (RanGAP) and the system is reset (reviewed in Macara, 1999). The significance of the NTF2-like domain, in the G3BPs, is unclear

but may suggest that these proteins shuttle from the cytoplasm to the nucleus in a fashion similar to NTF2. This data derived from the sequence analysis, suggest that the G3BPs belong to a superfamily of RNA-binding proteins functioning as regulators of RNA stability and/or transport.

Here, we report the cloning and characterization of mouse G3BP-1 as well as the identification of two alternatively spliced homologues of both mouse and human G3BP-2. We have also chromosomally mapped human G3BP-1 and G3BP-2, which map to 5q14.2-5q33.3 and 4q12-4q24, respectively. The primary sequence analysis of G3BP-1 reveals that it contains two minimal potential SH3 domain-binding motifs [Lee et al., 1996], whereas human G3BP-2a and G3BP-2b contain five and six, respectively. Recent in vivo data has shown that G3BPs bind to *ras*GAP^{120} [Parker et al., 1996; Gallouzi et al., 1998] however, the interactive regions of G3BP-1 and G3BP-2 have not yet been mapped. We have used bead-binding assays to map these regions, and identified the NTF2-like domain of both G3BP-1 and G3BP-2 as the *ras*GAP^{120} SH3-binding site.

MATERIALS AND METHODS

PCR and Subcloning

PCR reactions to amplify probes or for hybrid mapping, were carried out using 1.1 units of *Tth Plus* DNA Polymerase fragment (Biotech International) and buffer supplied by the manufacturer (Biotech International), and contained 100 ng template DNA and 50 pmol of each appropriate primer. Cycling conditions were: denaturation of DNA at 94°C for 1 min, annealing at 65°C for 1 min, and extension at 72°C for 1 min for 25 cycles.

Library Screening and Phage Isolation

Plasmid preparations, to be used as probes, library screening or sequencing, were made as described by Sambrook et al. [1989]. The libraries, late-primitive-streak stage mouse embryo cDNA [Kennedy et al., 1997], and a foetal human brain (cDNA kindly donated by Dr. T. Cox, University of Adelaide, Australia) were plated out at approximately 25,000 pfu/130 mm plate and duplicate filters (Hybond-N, Amersham) made from 21 plates. Library screening was performed, as described by Sambrook et al. [1989], with radioactive probes prepared using Amersham's Megaprime DNA labeling system according to the manufacturer's instructions. Hybridization conditions were as follows: 50% formamide, $5 \times$ SSC, 20 mM Tris-HCl, pH 7.6, $1 \times$ Denhardt's solution, and 0.1% SDS at 42°C. A minimum of 3×20 min washes of hybridized filters were performed in $0.2 \times$ SSC, 0.1% SDS at 65°C. cDNAs, from purified plaques, were subcloned into pBluescript SK (Stratagene).

Sub Cloning and Expression of Proteins Using Baculovirus

Full length cDNAs encoding for MmuG3BP-2a and 2b were excised from pBluescript using EagI (−85 bp from met start codon), and AccI (+140 bp from the stop codon), and subsequently end filled using Klenow fragment polymerase. These cDNAs were subcloned into SmaI linearised pBacPAK9 (Clontech), and transformed into competent DH5′a *E. coli* cells. The orientation of the inserts were checked by PCR. Plasmids, containing the inserts in the correct orientation, were transfected into *Spodoptera frugiperda* IPLB-Sf21 (Sf21) cells with Bsu36I digested BacPAK6 viral expression vector according to the manufacturer's instructions (Clontech #K1601-1). Recombinant virus plaques were selected from an Sf21 monolayer, and once again screened by PCR. Virus containing the coding cDNAs were amplified in Sf21 cells, and total cell lysates visualised on polyacrylamide gels for expression of proteins.

Total Protein Cell and Tissue Lysates

Cells and tissues were washed twice with ice cold phosphate-buffered saline (PBS), and solubilised or homogenised with a dounce homogeniser in HNTG lysis buffer consisting of 50 mM HEPES, pH 7.5, 150 mM NaCl, 1% Triton X-100, 10% glycerol, 1 mM $MgCl_2$, 1 mM EGTA, phosphatase inhibitors (1 mM Na_3VO_4, 10 mM $Na_4P_2O_7$, and 10 mM NaF), and protease inhibitors (1 μg of leupeptin per ml, 1 μg of trypsin inhibitor per ml, 1 μg of pepstatin A, 2 μg of aprotinin per ml, 10 μg benzamidine per ml, 1 mM phenylmethylsulfonyl floride, 1 μg of antipain per ml, 1 μg of chymostatin per ml). Lysates were cleared by centrifugation at 15,000 rpm for 10 min and the protein concentration determined by the Bradford dye-binding procedure using Bio-Rads Protein Assay (# 500-0001).

Fusion Protein Constructs and Expression

Truncated cDNAs representing either N-terminal or C-Terminal sequences of G3BP-1 and G3BP-2a (Fig. 2) were subcloned into bacterial GST-fusion expression vectors (pGex, Pharmacia) so that the recombinant fusion proteins could be expressed and used in bead binding assays (see below) to identify the sub-domains of G3BP that interact with the SH3 domain of rasGAP^{120}. The vectors containing the recombinant fusion protein construct were transformed into competent DH5′ *E.Coli* and expressed by IPTG induction. To collect the recombinant proteins, the cells were washed and resuspended in PBS, and sonicated to release the fusion proteins.

The N-terminal domain of *ras*GAP^{120} (kindly provided by Prof. I.G. Macara, University of Virginia) containing amino acids 1–356, which includes the full SH3 domain of *ras*GAP^{120} was subcloned into proEX HT bacterial expression vector (Life Technologies) and expressed as described above.

Bead Binding Assays

Glutathione columns (Pharmacia) were blocked overnight at 4°C in 1 × binding buffer A (50 mM HEPES, pH 7.4, 100 mM NaCl, 5 mM $MgCl_2$, 50 mg/ml BSA, 1 mM DTT, 1 mM PMFS, and protease inhibitors (Protease inhibitor cocktail, Roche Diagnostics, Australia). The following day the columns were washed twice with binding buffer A. Bacterial lysates containing either expressed GST alone or GST fusion proteins were diluted 1:1 with 2 × binding buffer A, and added to the equilibrated GST columns, the columns were gently rocked overnight at 4°C. To remove excess proteins the columns were washed twice in 1 × binding buffer A. Bacterial lysates containing the His-tagged N-terminal of rasGAP^{120} protein were combined with an equal volume of 2 × binding buffer A containing 200 mg/ml BSA and 0.1% Tween. In addition to the high concentration of BSA, which is used to block non-specific protein–protein interactions, Ethidium bromide was added to a final concentration of 25 ng/ml to abrogate non-specific interactions, caused by excess bacterial genomic DNA and bacterial RNA. This mix was then added to the pre-bound GST columns (above) and allowed to bind for 2 h at 4°C. The columns were then washed three times with binding buffer B (50 mM HEPES, pH 7.4, 200 mM NaCl, 5 mM $MgCl_2$, 1 mM DTT, 1 mM PMFS, and protease inhibitors).

Western Analysis of Protein–Protein Interactions

One microliter of the GST beads complexed with proteins, as described above, was added to an equal volume of 2 × PAGE loading dye, heated for 5 min at 95°C and loaded onto a 7.5% polyacrylamide gel and run at 100 V for 3 h. The proteins were transferred to nitrocellulose and probed with anti-His antibodies (Tetra-His antibody, Qiagen). Columns, which were bound with GST alone, were used as negative controls to ensure no non-specific His-tagged N-terminal rasGAP^{120} remained associated with the columns. To ensure that the GST columns had been saturated with the appropriate GST-G3BP peptides all experiments were probed with anti-GST to confirm that the columns contained the "bait" peptide (data not shown).

Protein Purification

A total of 500 ml of Sf21 cells, of at a concentration of 1.2–2.0 × 10^6 cells/ml, were infected with 60 ml of baculovirus (6.6 × 10^8–1.6 × 10^9 pfu/ml) containing cDNAs for expression of proteins and incubated at 28°C for 4 days in an orbital incubator. The cells were harvested and washed twice at 4°C with PBS, lysed in 50 ml of HNTG lysis buffer by 30 s vortexing and gentle rocking for 30 min at 4°C and cleared by centrifugation at 9,500 rpm × 10 min at 4°C. The final salt concentration was adjusted to 30 mM NaCl by addition of NaCl free and triton X-100 free HNTG lysis buffer (containing protease inhibitors), and incubated overnight on a rotating mixer at 4°C with pre-equilibrated heparin sepharose CL-6B (Pharmacia Biotech #17-0467-01) at a concentration of 15 mg of protein/ml of heparin sepharose. The gel was washed in 50 mM HEPES, pH 7.5, 10% glycerol and packed into a column (Pharmacia XK-26). The column was subjected to a 30 mM–1.0 M NaCl gradient over 120 min at a flow rate of 0.83 ml/min using a Pharmacia FPLC system. 1.5 ml samples were collected and assayed for MmuG3BP by separation on polyacrylamide gels and visualised by coomassie blue staining or western analysis using the 663 antibody.

Fractions containing the recombinant G3BP proteins were pooled and again diluted to a final

60 mM NaCl concentration. The pooled samples were incubated with agarose-polyribouridylic acid AGPoly(U), type 6 (Pharmacia Biotech #27-5535) at a concentration of 1.5 mg of protein/ml of gel overnight at 4°C on a rotating mixer. The following morning the gel was washed with 50 mM HEPES, pH 7.5, 10% glycerol, packed into a glass column (Pharmacia XK-16), and subjected to a 60 mM–1 M NaCl gradient at a flow rate of 0.33 ml/min as described above. A total of 0.5 ml fractions were collected, assayed, and pooled. Pooled samples were diluted to 30 mM NaCl and loaded onto a mono S HR 5/5 ion exchanger column (Pharmacia #17-0547-01) at a flow rate of 0.3 ml/min, and subjected to a 30 mM–1 M NaCl gradient. As described above, 0.5 ml fractions were collected and assayed.

Polyclonal Antibody Production

Affinity purified antibodies to G3BP-2 were obtained from an antiserum raised against an internal peptide sequence (SATPPPAEPASLP-QEPPKPRV). Polyclonal antibodies raised against G3BP-1 have been described elsewhere [Parker et al., 1996].

Western Blotting

Proteins were fractionated by sodium dodecyl sulfate (SDS)-polyacrylamide gel electrophoresis (7.5% gel) using the method of Laemmli and transferred onto polyvinylidene difloride (PVDF) membrane (Millipore Corp.) in a Bio-Rad trans-blot cell using a transfer buffer containing 25 mM Tris, pH 8.3, 192 mM Glycine, and 15% methanol. Electroblotting was carried out at 100 volts overnight at 4°C. The blot was blocked by incubation in 20 mM Tris-HCl, pH 7.5, 150 mM NaCl, 0.1% Tween-20, containing 10% skim milk (blocking solution) at room temperature for 1 h, followed by incubation with the primary antibody, anti-G3BP-1 (diluted 1:500) or anti-G3BP-2 (diluted 1:4,000) in blocking solution, at 4°C overnight. The blot was washed three times in blocking solution for 10 min, and subsequently incubated for 2 h at 37°C in the secondary antibody, which was an anti-rabbit conjugated with horseradish peroxidase (BioRad), diluted 1:10,000 in blocking solution.

Immunohistochemistry

Frozen mouse tissue sections (10 μm thickness) were fixed to Histogrip treated slides (SuperFrost Plus microscope slides, Menzel-Glaser, Germany), and air-dried overnight at room temperature. Sections were fixed for 5 min in 50% Chloroform, 50% Acetone, air dried, and rehydrated in Tris-buffered saline (TBS) (25 mM Tris, 137 mM NaCl, pH 7.4). Non-specific antibody binding was inhibited by incubation with TBS containing 4% skim milk powder for 15 min followed by an additional 20 min incubation in TBS, containing 10% normal goat serum (Gibco). Sections were then incubated overnight with either anti-G3BP-1 (diluted 1:300) or an anti-G3BP-2 (diluted 1:2,000). Excess antibody was removed by washing in TBS (3×5 min) and prediluted horseradish peroxidase (HRP) labeled anti-rabbit immunoglobulins (Envision) was applied for 30 min. Sections were then washed with TBS (3×5 min) and colour was developed in 3,3′-diaminobenzidine with H_2O_2 (Zymed) as a substrate for 2 min. Sections were washed with gently running tap water for 10 min to remove excess chromogen, lightly counterstained in Mayers' haematoxylin, dehydrated through ascending graded alcohols, cleared in xylene, then mounted using DPX [Harlow and Lane, 1988].

Fluorescence In Situ Hybridization of PACs

Fluorescence in situ hybridization was performed on peripheral human metaphase chromosomes. PAC DNA was biotin-14dATP-labelled by nick translation using the BioNick labeling system (Life Technologies). Chromosome preparation and FISH conditions were as described previously [Wicking et al., 1995]. Slides were analysed using an Olympus BH2 fluorescent microscope.

Chromosomal Mapping

Two HsaG3BP-1 specific primers, 5′ GGAGG-CATGGTGCAGAAACCA and 5′ CAGGAAAG-GGAAGAGAGGGAG and two HsaG3BP-2 specific primers, 5′ GTCTTGGCAGTGGTAC-ATTAT and 5′ AGTTCACTTTGTCGTAGA-TAGTTTAAG were used to amplify specific templates from human genomic DNA, and were subsequently used on the Genebridge4 Hybrid panel to identify positives. This data was then processed by the online mapping software available through the Whitehead Institute/MIT Center for Genome Research (http://carbon.wi.mit.edu).

RESULTS

Cloning, Sequence Homology, and Structural Homology

Previously, we reported the cloning of MmuG3BP-2 (MMU65313) in a general PCR-based screening for RRM-containing proteins [Kennedy et al., 1997]. This was achieved by using degenerate primers designed to consensus sequences within the RRM [Birney et al., 1993], and using the amplified PCR product to screen a late-primitive-streak stage mouse embryo cDNA library to isolate a full-length cDNA. Due to the highly conserved sequence homology between the G3BP genes, the coding region of the MmuG3BP-2 cDNA can be used as a useful tool to recognize both human G3BP-2, and MmuG3BP-1 in Northern analysis and library screening. We used the coding region of MmuG3BP-2 to isolate and clone MmuG3BP-1 (MMAB1927) and human G3BP-2 (HsaG3BP-2) from the late-primitive-streak stage mouse embryo cDNA library, and a foetal human brain cDNA library, respectively. The clones were sequenced and analysed to identify Met start codons, open reading frames and stop codons. Protein sequence comparison (Fig. 1) between HsaG3BP-2 and MmuG3BP-2 show 98.5% identity, HsaG3BP-2 and HsaG3BP-1 (HS3251910) show 65% identity and HsaG3BP-1 shares 94.4% sequence identity with MmuG3BP-1.

Screening of the libraries also revealed that (at least) two different isoforms of G3BP-2 are produced in both mouse and human. The alternative splicing event, which is 100% conserved between mouse and human, removes 99 nucleotides from the coding region, and does not introduce any stop codons or a frame shift. Both these transcripts are translated in vivo as was confirmed by Western analysis and recombinant protein expression (see below). We have designated the longer isoform G3BP-2a (human G3BP-2a accession number AF145285, mouse G3BP-2a accession number AF145285). The shorter protein isoform, which is referred to as G3BP-2b (human G3BP-2b accession number AF053535 and AF051311, and mouse G3BP-2b accession number MMU65313) differs from G3BP-2a by a 33 amino acid deletion from the central region of the primary structure (Fig. 1). We also detected and cloned a third transcript of MmuG3BP-2 (tentatively called G3BP-2c) however, sequence analysis indicated that translation of this transcript would lead to a truncated gene product, and so far, no corresponding protein has been detected in cells or tissues suggesting that it may not be translated.

All G3BPs share highly conserved RNP-1 and RNP-2 sequences, which are consensus motifs of RRMs. The most notable difference between G3BP-2 and G3BP-1 RRMs is a Val to Ile substitution in the RNP-2 consensus sequence (Fig. 1). The structure of the G3BP RRM has been reported elsewhere [Kennedy et al., 1997]. In addition, the G3BPs contain a conserved acid-rich domain and an RGG domain [Birney et al., 1993], both of which are commonly found in RNA-binding proteins. It should be noted that there are considerable differences in the RGG domain structure between G3BP-1 and G3BP-2 (see Fig. 1) and this may result in a different RNA target specificity. Although acid-rich domains are found in association with a variety of RNA-binding proteins such as hnRNP C and nucleolin, the function of this domain remains unclear and maybe involved in protein–protein interactions. The most significant difference between the G3BP-1 and G3BP-2 proteins lies in the number of potential SH3 domain-binding motifs (PxxP, where x represents any amino acid) [Lee et al., 1996]. The G3BP-2a protein contains a cluster of four PxxP motifs between the acid-rich and RRM domains, whereas G3BP-2b contains five in the homologous region (Fig. 1). The additional proline-rich PxxP motif in G3BP-2a is generated by the 33 amino acids spliced out of G3BP-2a. In contrast to the multiple PxxP, clusters found in G3BP-2s, G3BP-1 contains only one such motif in the homologous region of the protein (Fig. 1). Furthermore, both G3BP-1 and G3BP-2 contain a conserved PxxP motif (PGGP) within their non-conserved RGG domains (Fig. 1). The specific conservation of the minimal SH3 domain-binding motif within a region of the protein, which is generally not conserved, may suggest a retained function, although this remains to be determined. The overall differences in the number of potential SH3 domain-binding motifs between the G3BPs may indicate that in vivo they may bind different SH3 domain-containing partners or have different affinities for the same protein.

Chromosomal Location of G3BPs

Sequence data, obtained from the library clones, was used to design G3BP-1 and G3BP-2 specific primers, which were subsequently used

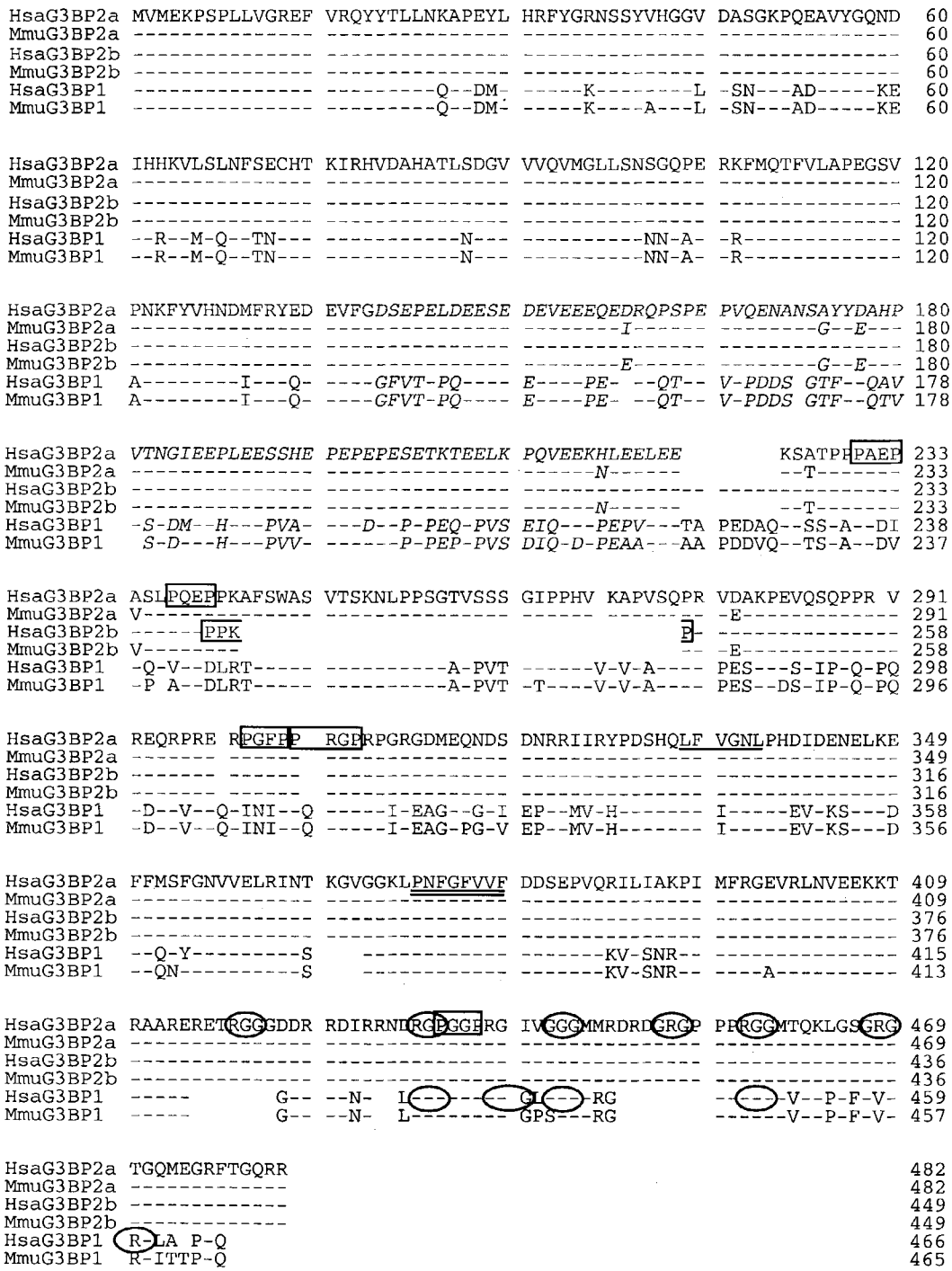

Fig. 1. Clustal alignment of the G3BP family of proteins. Amino acids are shown in single letter format and grouped in blocks of 10. Numbering at the end of the line indicates the amino acid position within the indicated protein. Dashes within the aligned sequences indicate conserved amino acids with respect to HsaG3BP-2a; amino acid changes between proteins have been indicated by the appropriate substitution. Spaces within the aligned proteins indicate gaps inserted into the sequences to maintain co-linearity. Boxes represent proline rich sequences (PxxP). Sequences in italics indicate the acid-rich domain. Ovals represent components of an RGG domain; note that the RGG domains of G3BP-1 and G3BP-2 are divergent. Underlined and double underlined sequences indicate RNP-2 and RNP-1, respectively.

on the GeneBridge hybridisation panel to determine the chromosomal localisation of these genes. G3BP-1 mapped to chromosome 5 at 1.51 cR from FB25D10 (lod > 3.0), which places the gene between 5q33.1-5q33.3. G3BP-2 mapped to chromosome 4 at 3.36 cR from WI-5565 (lod > 3.0), which places the gene between 4q12-4q24. We subsequently screened a plasmid artificial chromosome (PAC) library (kindly donated by Dr. P. Ioannou, The Murdoch Institute, Australia) and used the isolated clones to perform fluorescent in situ hybridization. The results of the FISH confirmed the genetic location of these genes. In addition to screening the GeneBridge hybridization panel and the FISH analysis, the human genome sequences in the NCBI databases (http://www.ncbi.nlm.nih.gov/genome/seq/) were BLAST searched with the cDNA sequences of human G3BP-1 and G3BP-2. The results indicated that there are several chromosomes with matches to either G3BP-1 or G3BP-2, which may represent gene duplications or pseudo-genes. The BLAST analysis on its own was not sufficient to map the G3BPs however, in conjunction with the FISH and the GeneGridge hybridisation panel results the chromosomal localisation of these genes as indicated above has been confirmed.

A search of the genomic databases (available at http://gdbwww.gdb.org/gdbreports/GeneByChromosome.4.alpha.html and http://gdbwww.gdb.org/gdbreports/GeneByChromosome.5.alpha.html) did not reveal any candidate loci for diseases that may represent genetic defects/polymorphisms in this family of proteins, although, there does appear to be some clustering of RNA-binding protein genes on chromosome 5q including, hnRNP A/B (GDB:128837), hnRNP H1 (GDB:5428597), ribosomal protein L7 pseudo gene (GDB:277889), ribosomal protein S14 (GDB:119572), ribosomal protein S17a-like 1 (GDB:119573), ribosomal protein S20A (GDB:119575), and ribosomal protein S20B (GDB:119576). Chromosome 4q also contains several RNA-binding proteins including EIF4EL1 (GDB:126371), G-rich RNA sequence binding factor 1 (GDB:696354), hnRNP D (GDB:9391694), RNA polymerase II polypeptide B (GDB:135034), and ribosomal protein L34 (GDB:9863242). Segment deletions and breakpoint analysis of regions overlapping the chromosomal location of G3BP-1 suggest that this region may be involved in myeloid leukemias [Horrigan et al., 1999], whereas similar studies for chromosome 4q suggest the region containing the G3BP-2 gene may be involved in colorectal adenoma [Wong et al., 1999], and Hodgkin disease [Atkin, 1998]. However, there is insufficient data to suggest that any G3BPs are involved in human pathologies that are linked to these regions of the human chromosomes.

Protein Expression in Insect Cells

MmuG3BP-2a and 2b cDNAs encode proteins, whose predicted sizes are 58.2 and 54.9 kDa, respectively. The expressed recombinant proteins have apparent molecular weights of 68.5 and 62 kDa, respectively, as determined by SDS–PAGE (data not shown). These differences in predicted and apparent masses are consistent with an increase in mass due to post translational modifications, and are similar to those reported for HsaG3BP-1 (predicted mass of 54.9, observed apparent mass of 68 kDa) [Parker et al., 1996].

Mapping of G3BP-*ras*GAP^{120} Interactions

Interactions between G3BP-1 and *ras*GAP^{120} have been reported and show that G3BP-1 specifically interacts with the SH3 domain of *ras*GAP^{120} [Parker et al., 1996] implicating G3BP in the *ras*GAP^{120} signal transduction pathway (see also Pazman et al., 2000). However, the region within the G3BPs responsible for the observed interaction with *ras*GAP^{120} has not been thoroughly investigated. Initially, it was presumed that the interactions would be facilitated through proline rich motifs that are known to interact with SH3 domains [Lee et al., 1996]. To further map the interactions between G3BPs and the SH3 domain of *ras*GAP^{120} several GST-G3BP peptide fusions were expressed (Fig. 2), and probed in bead binding assays with His-tagged N-terminal *ras*GAP^{120} peptides. The G3BP peptide constructs were designed to represent truncated proteins containing single or multiple domains as well as peptides that would contain isolated proline rich motifs (Fig. 2). In the assays, GST-G3BP peptides are bound to glutathione beads, and His-tagged N-terminal *ras*GAP^{120} is added to the different constructs. Specific protein–protein interactions between the G3BP peptides, and the SH3 domain of *ras*GAP^{120} are detected by running the bound proteins on a Western and identifying His-tagged *ras*GAP^{120} by probing

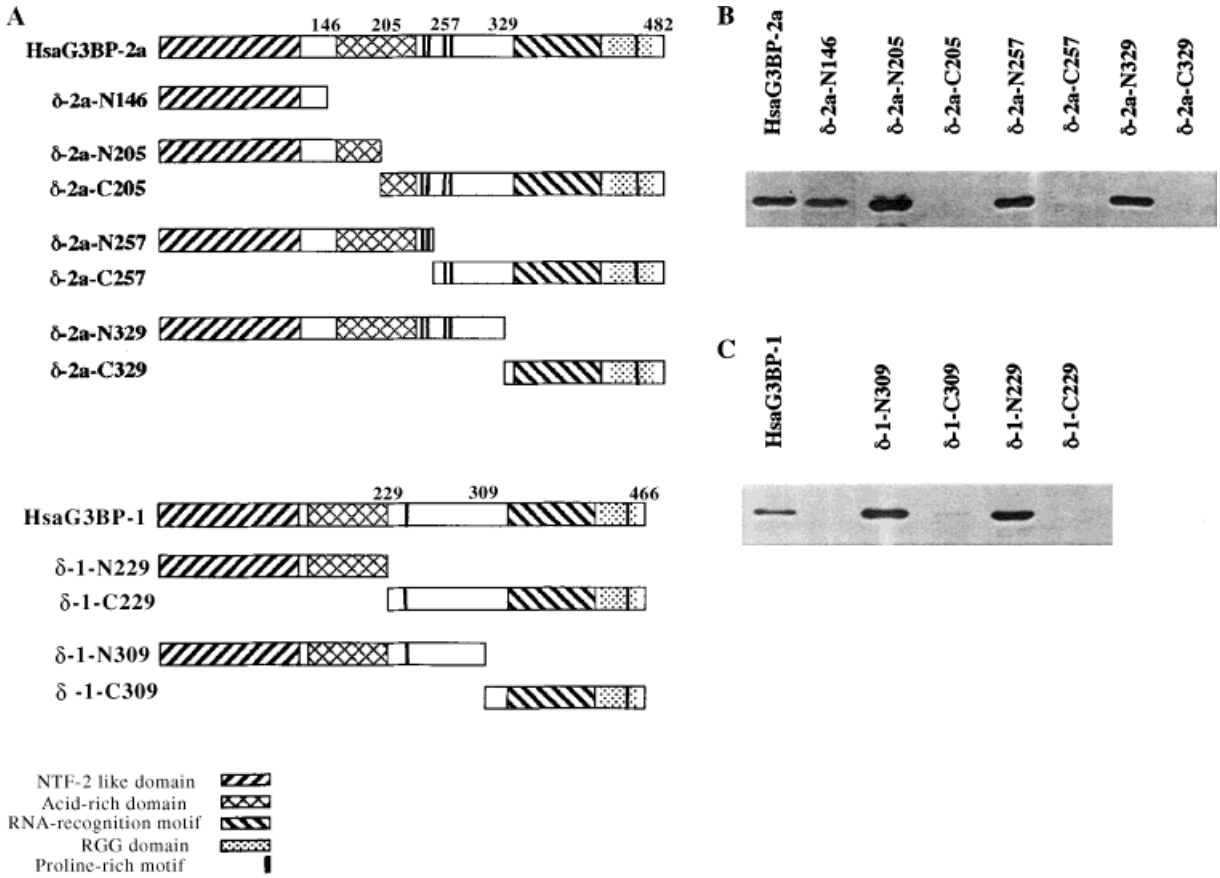

Fig. 2. Analysis of protein–protein interactions between the SH3 domain of N-terminal *ras*GAP^{120} and G3BP. **A:** Schematic representation of the sub-domains and motifs contained within the G3BP-2a and G3BP-1 proteins and includes the N-terminal NTF2-like, Acid-Rich, RGG, and proline-rich domains as well as the RNA-recognition motif (see insert for details). Below the respective full length proteins are shown the various truncated peptides that were expressed as GST-fusion proteins to map the interactions with the N-terminal SH3 domain containing region of *ras*GAP^{120}, the numbering corresponds to the amino acid at the site of the peptide truncation (i.e., δ-2a-N146 represents the truncated G3BP-2a peptide including the N-terminal amino acids 1–146), the relative position of these truncations is shown to approximate scale in the full length proteins. **B** and **C:** Western analysis of Glutathione beads bound with various GST-G3BP peptides, and probed with the His-tagged N-terminal SH3 domain containing region of *ras*GAP^{120}. G3BP- *ras*GAP^{120} interactions were determined by probing the Westerns with anti-His antibodies. The results show that the N-terminal SH3 domain containing region of *ras*GAP^{120} interacted with the NTF2-like domain of G3BP-2a (δ-2a-N146, panel B), and any peptide of G3BP-2a that contained the NTF2-like domain (δ-2a-N205, δ-2a-N257, δ-2a-N329, and full length G3BP-2a, panel B). The results obtained from G3BP-1 are consistent with these results from G3BP-2a and show that full length G3BP-1, δ-1-N229 and δ-1-N309 interact with the N-terminal SH3 domain containing region of *ras*GAP^{120}. Truncated peptides of either G3BP-2a or G3BP-1 that did not contain an intact NTF2-like domain failed to bind with the SH3 region of *ras*GAP^{120}.

with an anti-His antibody. The results show (Fig. 2) that the interaction between the SH3 domain of *ras*GAP^{120} maps to the NTF2-like domain contained within the N-terminal domain of the G3BPs, but not the proline rich motifs. No interactions were detected with the other domains of G3BP including the Acid-Rich domain, the RRM or the RGG-rich domain (Fig. 2). The results reported here were confirmed using far-Western protocols (data not shown) and are consistent with the data obtained from the bead binding assays.

G3BPs Have a Tissue Specific Expression

Antibodies raised against isoform specific synthetic peptides determined from G3BP-1 and G3BP-2 sequences were used to probe Western blots of total cell lysates from adult mouse tissues (Fig. 3). Figure 3, panel A shows tissues probed with anti-G3BP-1 polyclonal antibodies, whereas panel B shows a collage of tissues probed with anti-G3BP-2 polyclonal antibodies. Some tissues are shown to express both isoforms of G3BP-2 (Fig. 3, panel B)

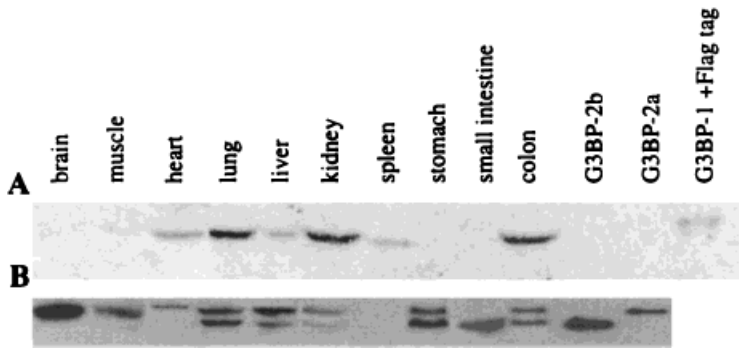

Fig. 3. Western blot analysis of G3BP expression. **Panel A** shows tissues probed with an anti-G3BP-1 antibody, whereas **panel B** shows tissues probed with an anti-G3BP-2 antibody. The upper bands in panel B show G3BP-2a, whereas the lower bands are the shorter G3BP-2b isoform.

including lung, liver, kidney, stomach, and colon (also pancreas and testis, data not shown). Other tissues are restricted to only expressing G3BP-2a (upper band in Fig. 3, panel B) including brain, muscle (small amount of G3BP-2b expression is seen, and is presumably caused by the presence of different cell populations within the sample), and heart. Small intestine expresses only MmuG3BP-2b (lower band Fig. 3, panel B), and spleen does not express either protein at detectable levels. Although, the general expression of the G3BP-1 antibody appears lower than that of G3BP-2, some tissues express abundant levels of G3BP-1 and include lung, kidney, and colon. Heart, liver, and spleen also express low levels of G3BP-1.

Immunohistochemistry

Immunohistochemistry was used to analyse in full detail, the degree of cell specificity of the G3BP-1 and G3BP-2 expression. Until isoform specific antibodies are raised against G3BP-2a and G3BP-2b, it is not possible to distinguish these isoforms in immunohistochemistry however, in some tissues we can specify, which isoform is being expressed by comparison to the Western data (above). Figure 4 shows a cross section of results from some of the tissues studied. Panels A–E are probed with anti-G3BP-1 antibodies, whereas panels F–J are probed with anti-G3BP-2 antibodies. Panels A and F show a comparison of adult mouse brain. As already determined by Western analysis (Fig. 3, panel A), brain does not express G3BP-1 (Fig. 4, panel A) however, a sub-population of cells express G3BP-2a (panel F). We determined by cell morphology and double staining with a neural marker (data not shown) that the G3BP-2a positive cells are neural cells (panel F, labeled Ne), and that the negative cells are glial cells (panel F, labeled Gl). In the kidney (panels B and C), G3BP-1 appears to be expressed in interstitial cells or a sub-population of tubules (panel B), whereas G3BP-2 is expressed at low levels in all tubules (labeled Tu in panel G). Neither G3BP-1 nor G3BP-2 are expressed in the glomerulus (labeled Gm in panel G). The colon (panels C and H) shows that G3BP-1 is expressed at the periphery of the intestinal glands or possibly in interstitial cells, whereas G3BP-2 is expressed in the lumen of the intestinal glands (labeled Ig in panels H and I). G3BP-2 is also expressed at high levels in the villi of the small intestine (Fig. 4 panel I), whereas G3BP-1 (Fig. 4, panel D) was not detected at levels above the background staining of the negative control. Once again, no detectable staining was observed for G3BP-1 in stomach (Fig. 4, panel E), whereas G3BP-2 (presumably G3BP-2b only from the Western data) appears to be expressed in the mucus secreting cells of the stomach lumen (labeled Ep in panel J), and the internal surface of the pyloric glands (labeled Pg in panel J). Other tissues examined by immunohistochemistry include heart, liver, and spleen (data not shown). Heart and liver showed a general low level expression of G3BP-1 and G3BP-2, whereas spleen was negative for G3BP-2 and showed a cell specific staining of G3BP-1. It is still to be determined what types of cells constitute the G3BP-1 expressing islands observed within the spleen.

DISCUSSION

Src homology 3 domains were initially characterized in signal transduction proteins such as

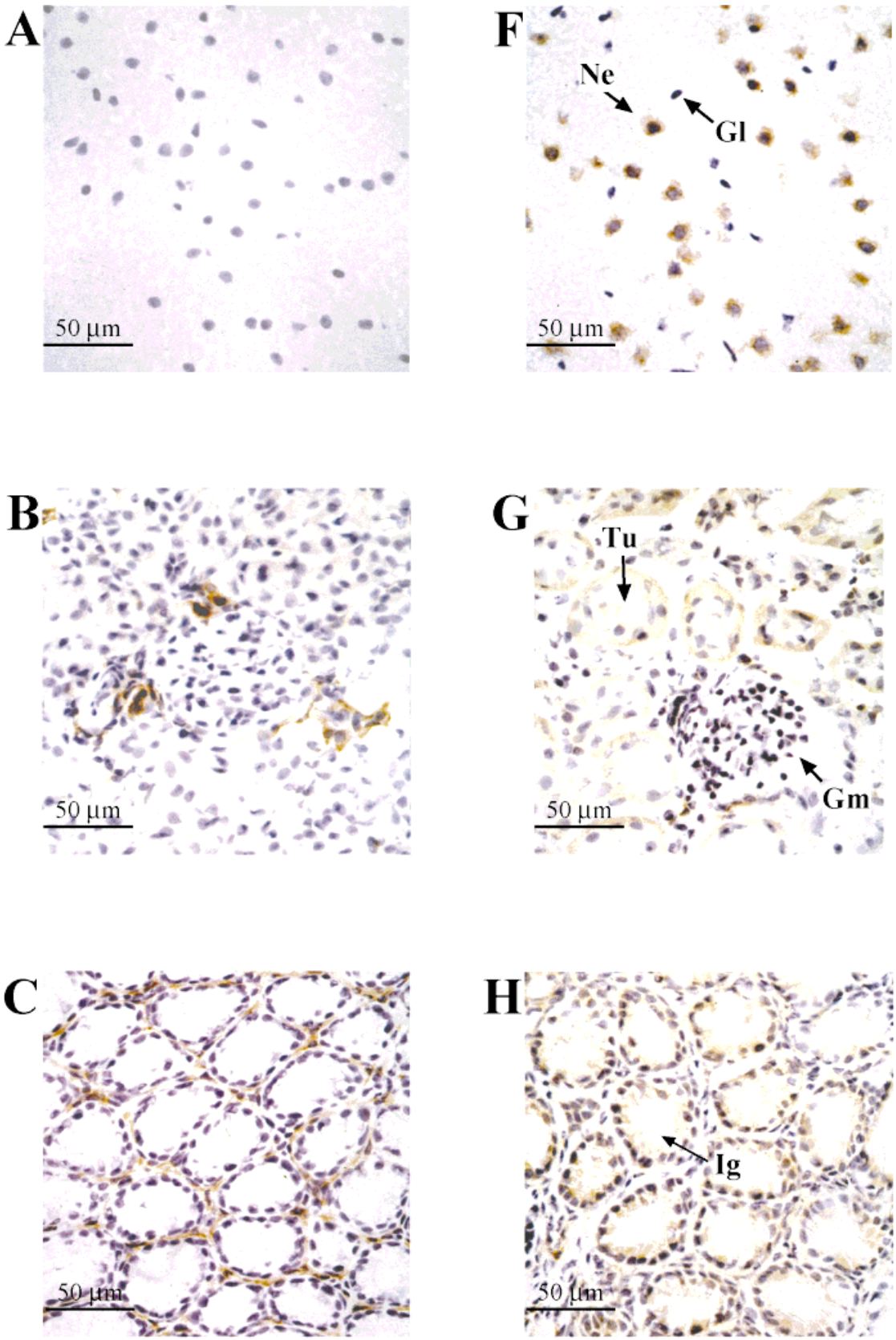

Fig. 4. (*Continued*)

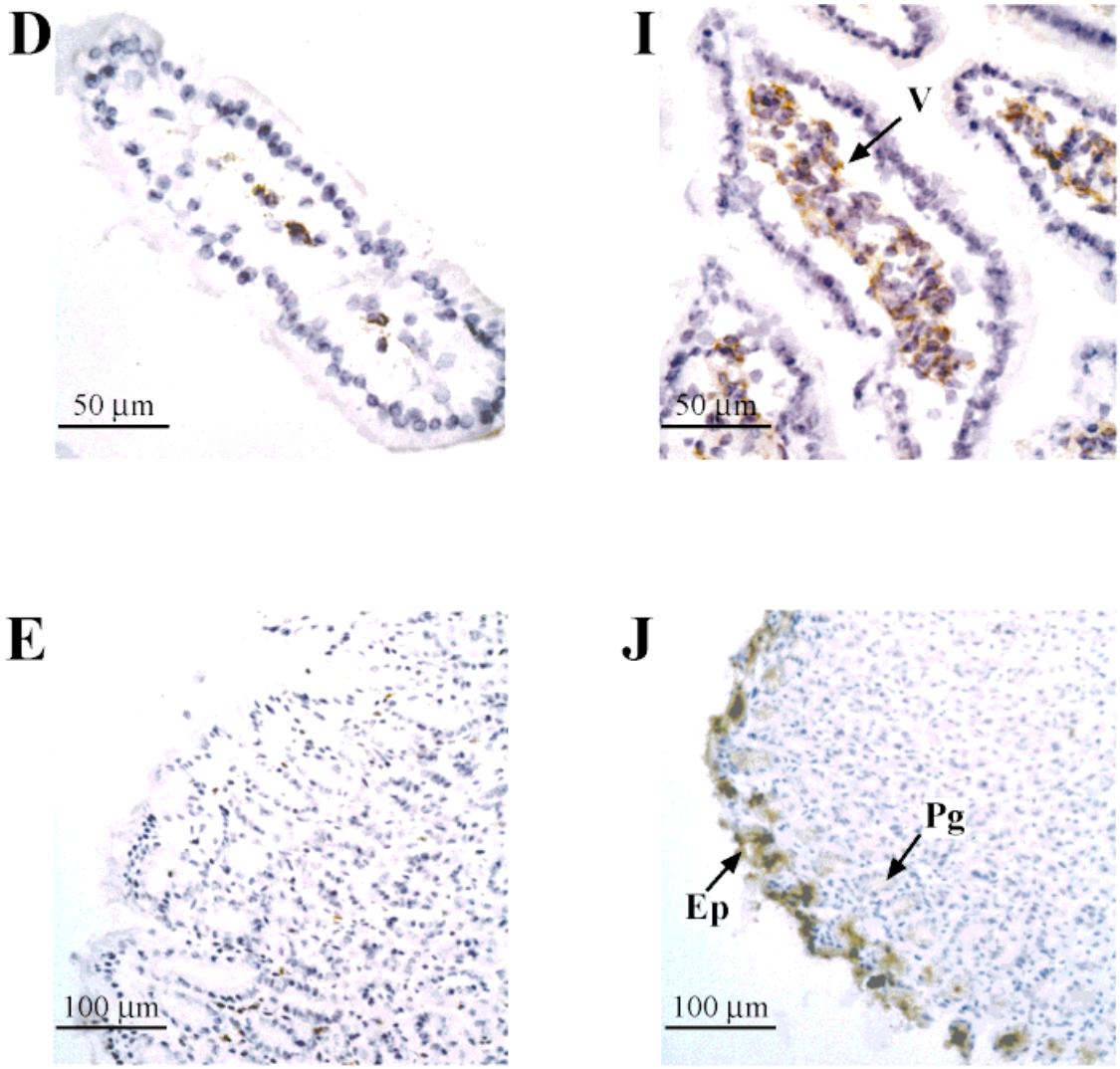

Fig. 4. Immunohistochemistry of adult mouse tissues. **Panels A–E** are probed with an anti-G3BP-1 antibody, whereas **panels F–J** are probed with an anti-G3BP-2 antibody, all tissue staining was visualised with horse radish peroxidase, and sections were counterstained with haematoxylin. Panels A and F are brain (Ne denotes a neurone, Gl denotes a glial cell), B and G are kidney (Gm denotes a glomerulus, Tu denotes a tubule), C and H are colon (lg denotes an intestinal gland), D and I are small intestine (V denotes a villi), and E and J are stomach (Ep denotes epithelial mucus secreting cells and Pg denotes a pyloric gland). All photographs are taken at 100 × magnification (bars represent 100 µm) with the exception of stomach (panels E and J), which is displayed at 50 × magnification (bars represent 100 µm).

Src, Fyn, and Grb as well as *ras*GAP^{120}. Typically, these domains interact with proline rich motifs with a minimum consensus of PxxP however, other non-canonical binding interactions have been reported [Urquhart et al., 2000]. G3BP-1 has two PxxP sequences that could putatively bind with the SH3 domain of *ras*-GAP^{120}, whereas G3BP-2a has up to five PxxP sequences (Fig. 2). Primary sequences of G3BP-2a and G3BP-2b suggested that the additional minimal SH3 binding-domain generated in G3BP-2b by an alternative splicing event may represent a control mechanism for signal transduction through proteins such as *ras*GAP^{120}, and thereby represent a means of controlling RNA metabolism. Experiments, reported here, were designed to map the region of G3BPs that interacts with the SH3 domain of *ras*GAP^{120} and were initially directed at determining, which proline-rich region was responsible for the interactions reported elsewhere through co-immunoprecipitation experiments or genetic interactions [Parker et al., 1996; Pazman et al., 2000]. It was surprising that the smallest

G3BP truncated protein that was capable of binding to the SH3 domain of *ras*GAP^{120} did not contain any of the predicted PxxP motifs normally associated with SH3 binding. The results of these protein interactions clearly show that the N-terminal NTF2-like domain of G3BP is responsible for the binding interactions with N-terminal *ras*GAP^{120}. This is an unexpected result, and the significance of this interaction is unclear; it would be tempting to speculate that this interaction may somehow influence the movement of G3BP in or out of the nucleus. However, there is little evidence to connect *ras*GAP^{120}-G3BP interactions with nuclear transport, and the biological consequences of this interaction will need to be elucidated.

Recent evidence suggests that tyrosine kinase pathway-based signal transduction may also connect to RNA through SH2 and SH3 domain-binding proteins [Hobert et al., 1994]. The RNA-binding protein hnRNP K has been shown to bind the SH3 domain of p95^{vav} with downstream responses/activity occurring in the cytoplasm and nucleus [Hobert et al., 1994]. Along with another RNA-binding protein, Sam68 [Barlat et al., 1997], this activity describes a novel signaling pathway acting at the level of RNA processing. G3BP-1 and G3BP-2s interact with the SH3 domain of *ras*GAP^{120}, as shown previously in vivo [Parker et al., 1996; Gallouzi et al., 1998], and by protein–protein analysis, reported here, implicating these proteins in signal transduction. These proteins are unlikely to act in the same mode as hnRNP K or Sam68 as G3BPs are RRM-type RNA-binding proteins, whereas hnRNP K and Sam68 contain a KH motifs [Hobert et al., 1994; Barlat et al., 1997], suggesting they are members of a separate family of proteins.

Western and immunohistochemistry show that G3BPs are expressed in a tissue and cell-specific manner. In the brain, the expression of this family of proteins is strictly limited to G3BP-2a in the neurones with no other family members expressed in the brain. Conversely, for the small intestine, G3BP-2b is expressed exclusively in the lumen of the villi. The fact that some tissues express all family members (i.e., lung, liver, stomach, and colon), whereas other tissues are almost devoid of their expression (i.e., spleen), suggests that these tissues may have distinct populations of RNAs that require specific metabolism regulated through signal transduction pathways that involve factors such as *ras*GAP^{120} and/or other SH3-containing protein partners.

The data presented here shows that G3BP-1 and G3BP-2 are related, but distinct proteins as demonstrated by their divergent primary sequences and chromosomal locations. While these proteins may carry out similar biochemical functions, the reported differences in subcellular localisation [Parker et al., 1996; Costa et al., 1999] and tissue specific protein expression suggest that their biological role is distinct. Members of the RRM-containing family of proteins are involved in RNA transport between the nucleus and the cytoplasm [Piñol-Roma and Dreyfuss, 1992; Dreyfuss et al., 1996], and some members of the family are involved in DNA-binding [Johnston et al., 1999], which has lead to the speculation that these proteins may act as transcription factors [DeAngelo et al., 1995]. The activity of an RRM-containing protein may therefore dictate its sub-cellular distribution. The nuclear and cytoplasmic location of G3BPs suggests that this family of proteins may be involved in signaling to nuclear RNA/DNA targets or regulating nuclear shuttling of mRNAs and that the different members of the G3BP family target separate DNA/RNA targets. It is equally possible that although the G3BP proteins share a high degree of homology that their functions are quite different. In vitro activity of G3BP-1 suggests that it may act as an RNAase [Gallouzi et al., 1998] or a helicase [Costa et al., 1999], but no such functions have been attributed to G3BP-2 and the characterization of the proteins functions will need further analysis, which is currently being conducted.

Based on the evidence presented here and elsewhere [Parker et al., 1996; Gallouzi et al., 1998], we propose that the G3BP family of proteins are *bona fide* RNA-binding and SH3 domain-binding proteins, and are possibly regulated by signal transduction downstream of *ras*GAP^{120} or other SH3-containing proteins. G3BP-1 and G3BP-2s are members of a novel sub-class of the RNA-binding protein superfamily that act at the level of RNA metabolism in response to cell signaling, possibly as RNA transcript stabilising factors or an RNAase [Gallouzi et al., 1998]. This form of cell signaling, influencing transcript stability, would provide cells with the mechanism for intermediate control of gene expression, somewhere

between transcriptional regulation and post-translational modification of proteins in response to external signals. This would prove to be a more direct and dynamic response than is possible with more medium term control of de novo gene transcription.

ACKNOWLEDGMENTS

We thank Nyoman Kurniawan, Jenny Cassady, and Emma Puttick for their assistance in DNA sequencing, and Li-Chen Zhang for her invaluable technical support. We also like to thank Drs. P. Ioannou and D. Beck for allowing us to use their PAC library as well as Kylie Negus, and Dr. G. Chenevix-Trench for their assistance and analysis of human chromosomes for FISH. The Centre for Molecular and Cellular Biology is a Special Research Centre of the Australian Research Council. Juliet French is supported by an Australian Postgraduate Award.

REFERENCES

Atkin NB. 1998. Cytogenetics of Hodgkin disease. Cytogenet Cell Genet 80:23–27.

Barlat I, Maurier F, Duchesne M, Guitard E, Tocque B, Schweighoffer F. 1997. A role for Sam68 in cell cycle progression antagonized by a spliced variant within the KH domain. J Biol Chem 272:3129–3132.

Birney E, Kumar S, Krainer AR. 1993. Analysis of the RNA-recognition motif and RS and RGG domains: conservation in metazoan pre-mRNA splicing factors. Nucleic Acids Research 21:5803–5816.

Bopp D, Calhoun G, Horabin JI, Samuels M, Schedl P. 1996. Sex-specific control of *Sex-lethal* is a conserved mechanism for sex determination in the genus *Drosophila*. Development 122:971–982.

Burd CG, Dreyfuss G. 1994. Conserved structures and diversity of functions of RNA-binding proteins. Science 265:615–621.

Costa M, Ochem A, Staub A, Falaschi A. 1999. Human DNA helicase VIII: a DNA and RNA helicase corresponding to the G3BP protein, an element of the Ras transduction pathway. Nucl Acids Res 27:817–821.

Crozat A, Aman P, Mandahl N, Ron D. 1993. Fusion of CHOP to a novel RNA-binding protein in human myxoid liposarcoma. Nature 363:640–644.

DeAngelo DJ, DeFalco J, Rybacki L, Childs G. 1995. The embryonic enhancer-binding protein SSAP contains a novel DNA-binding domain which has homology to several RNA-binding proteins. Mol Cell. Biol 15:1254–1264.

Dreyfuss G, Hentze M, Lamond AI. 1996. From transcript to protein. Cell 85:963–972.

Duchesne M, Schweighoffer F, Parker F, Clerc F, Frobert Y, Thang MN, Tocque B. 1993. Identification of the SH3 domain of GAP as an essential sequence for Ras-GAP-mediated signaling. Science 259:525–528.

Gallouzi IE, Parker F, Chebli K, Maurier F, Labourier E, Barlat I, Capony JP, Tocque B, Tazi J. 1998. A novel phosphorylation-dependent RNase activity of GAP-SH3 binding protein: a potential link between signal transduction and RNA stability. Mol Cell Biol 18:3956–3965.

Harlow E, Lane D. 1988. Antibodies a laboratory manual New York: Cold Spring Harbor Laboratory.

Hobert O, Jallal B, Schlessinger J, Ullrich A. 1994. Novel signalling pathway suggested by SH3 domain-mediated $p95^{vav}$/Heterogeneous Ribonucleoprotein K interaction. J Biol Chem 269:20225–20228.

Horrigan SK, Bartoloni L, Speer MC, Fulton N, Kravarusic J, Ramesar R, Vance JM, Yamaoka LH, Westbrook CA. 1999. A radiation hybrid breakpoint map of the acute myeloid leukemia (AML) and limb-girdle muscular dystrophy 1A (LGMD1A) regions of chromosome 5q31 localizing 122 expressed sequences. Genomics 57:24–35.

Hu K-Q, Settleman J. 1997. Tandem SH2 binding sites mediate the RasGAP-RhoGAP interaction: a conformational mechanism for SH3 domain regulation. EMBO J 16:473–483.

Johnston SD, Lew JE, Berman J. 1999. Gbp1p, a protein with RNA recognition motifs, binds single-stranded telomeric DNA and changes its binding specificity upon dimerization. Mol Cell Biol 19:923–933.

Kennedy D, Wood SA, Ramsdale T, Tam PP, Steiner K, Mattick JS. 1997. Identification of a mouse orthologue of the human ras-GAP-SH3-domain binding protein and structural confirmation that these proteins contain an RNA recognition motif. Biomedical. Peptides, Proteins and Nucleic Acids 2:93–99.

Leblanc V, Tocque B, Delumeau I. 1998. Ras-GAP controls Rho-mediated cytoskeletal reorganization through its SH3 domain. Mol Cell Biol 18:5567–5578.

Lee CH, Saksela K, Mirza UA, Chait BT, Kuriyan J. 1996. Crystal structure of the conserved core of HIV-1 Nef complexed with a Src family SH3 domain. Cell 85:931–942.

Liu YF, Deth RC, Devys D. 1997. SH3 domain-dependent asscociation of Huntingtin with epidermal growth factor receptor signaling complexes. J Biol Chem 272:8121–8124.

Macara IG. 1999. Nuclear transport: randy couples. Curr Biol 9:R436–R439.

Nagai K, Oubridge C, Ito N, Avis J, Evans P. 1995. The RNP domain: a sequence-specific RNA-binding domain involved in processing and transport of RNA. Trends Biochem Sci 20:235–240.

Parker F, Maurier F, Delumeau I, Duchesne M, Faucher D, Debussche L, Dugue A, Schweighoffer F, Tocque B. 1996. A ras-GTPase-activated protein SH3-domain-binding protein. Mol Cell Biol 16:2561–2569.

Pazman C, Mayes CA, Fanto M, Haynes SR, Mlodzik M. 2000. Rasputin, the Drosophila homologue of the Ras-GAP SH3 binding protein, functions in ras- and Rho-mediated signaling. Development 127:1715–1725.

Piñol-Roma S, Dreyfuss G. 1992. Shuttling of pre-mRNA binding proteins between nucleus and cytoplasm. Nature 355:730–732.

Pomerance M, Thang MN, Tocque B, Pierre M. 1996. The ras-GTPase-activating protein SH3 domain is required for Cdc2 activation and Mos induction by oncogenic ras in *Xenopus* oocytes independently of mitogen-activated protein kinase activation. Mol Cell Biol 16:3179–3186.

Sakakibara S-I, Imai T, Hamaguchi K, Okabe M, Arunga J, Nakajima K, Yasutomi D, Nagata T, Kurihara Y, Uesugi S, Miyata T, Ogawa M, Mikoshiba K, Okano H. 1996. Mouse-*musashi-1*, a neural RNA-binding protein highly enriched in the mammalian CNS stem cell. Dev Biol 176:230–242.

Sambrook J, Fritsch EF, Maniatis T. 1989. Molecular Cloning A Laboratory Manual. Cold Spring Harbor: Cold Spring Harbor Laboratory Press.

Siomi H, Dreyfuss G. 1997. RNA-binding proteins as regulators of gene expression. Curr Opin Genet Dev 7: 345–353.

Siomi H, Siomi MC, Nussbaum RL, Dreyfuss G. 1993. The protein product of the fragile X gene, *FMR1*, has characteristics of an RNA-binding protein. Cell 74:291–298.

Suyama M, Doerks T, Braun IC, Sattler M, Izaurralde E, Bork P. 2000. Prediction of structural domains of TAP reveals details of its interaction with p15 and nucleoporins. EMBO rep 1:53–58.

Svitkin YV, Ovchinnikov LP, Dreyfuss G, Sonenberg N. 1996. General RNA binding proteins render translation cap dependent. EMBO J 15:7147–7155.

Tocque B, Delumeau I, Parker F, Maurier F, Multon C-M, Schweighoffer F. 1997. Ras-GTPase activating protein (GAP): A putative effector for ras. Cell Signal 9:153–158.

Tuteja R, Tuteja N. 1998. Nucleolin: a multifunctional major nucleolar phosphoprotein. Crit Rev Biochem Mol Biol 33:407–436.

Urquhart AJ, Kennedy D, Gould SJ, Crane DI. 2000. Interaction of Pex5p, the Type 1 Peroxisome Targeting Signal Receptor, with the Peroxisomal Membrane Proteins Pex14p and Pex13p. J Biol Chem 275:4127–4136.

van der Geer P, Henkemeyer M, Jacks T, Pawson T. 1997. Aberrant Ras regulation and reduced p190 tyrosine phosphorylation in cells lacking p120-Gap. Mol Cell Biol 17:1840–1847.

Wicking C, Breen M, Negus K, Berkman J, Evdokiou A, Cowled P, Chenevix-Trench G, Wainwright B. 1995. The human growth-arrest-specific gene GAS1 maps outside the candidate region of the gene for nevoid basal cell carcinoma syndrome. Cytogenet Cell Genet 68:119–121.

Wong N, Lai P, Lee SW, Fan S, Pang E, Liew CT, Sheng Z, Lau JW, Johnson PJ. 1999. Assessment of genetic changes in hepatocellular carcinoma by comparative genomic hybridization analysis: relationship to disease stage, tumor size, and cirrhosis. Am J Pathol 154:37–43.